AD-A120 906 NONSPHERICAL PARTICLE INVESTIGATION(U) BOEING AEROSPACE 1/1
CO SEATTLE WA C D CAPPS ET AL. SEP 82 NWSC/CR-RDTR-127
N00164-81-C-0206

UNCLASSIFIED F/G 20/8 NL

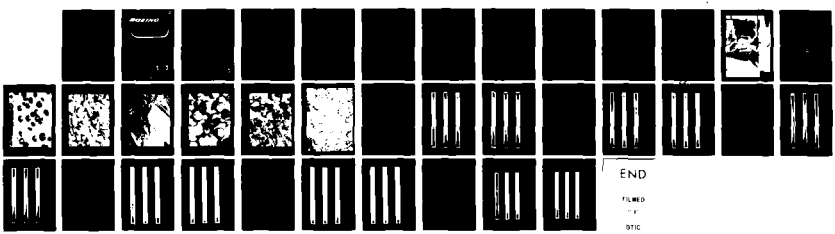

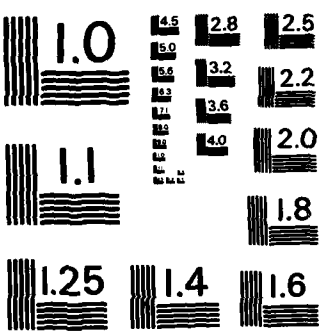

2

Final Report

Nonspherical Particle Investigation

Contract No. N00164-81-C-0206

Submitted to

United States Navy

Naval Air Systems Command

Washington, DC 20361

Approved for Public Release;
Distribution Unlimited

September 1982

Boeing Aerospace Company

Seattle, WA 98124

UNCLASSIFIED

SECURITY CLASSIFICATION OF THIS PAGE (When Data Entered)

REPORT DOCUMENTATION PAGE	READ INSTRUCTIONS BEFORE COMPLETING FORM
1. REPORT NUMBER: NWSC/CR/RDTR-127	2. GOVT ACCESSION NO.: AD-A120 706
	3. RECIPIENT'S CATALOG NUMBER
4. TITLE (and Subtitle): NONSPHERICAL PARTICLE INVESTIGATION	5. TYPE OF REPORT & PERIOD COVERED: Final Report Sept. 25, 1981-June 25, 1982
	6. PERFORMING ORG. REPORT NUMBER
7. AUTHOR(s): C. D. Capps, A. R. Tokuda, G.M. Hess	8. CONTRACT OR GRANT NUMBER(s): N00164-81-C-0206
9. PERFORMING ORGANIZATION NAME AND ADDRESS: Boeing Aerospace Company, P.O. Box 3999, Seattle, WA 98124	10. PROGRAM ELEMENT, PROJECT, TASK AREA & WORK UNIT NUMBERS: PE 61153N
11. CONTROLLING OFFICE NAME AND ADDRESS: Naval Weapons Support Center, Crane, Indiana 47522	12. REPORT DATE: September 1982
	13. NUMBER OF PAGES: 35
14. MONITORING AGENCY NAME & ADDRESS (if different from Controlling Office)	15. SECURITY CLASS. (of this report): UNCLASSIFIED
	15a. DECLASSIFICATION/DOWNGRADING SCHEDULE

16. DISTRIBUTION STATEMENT (of this Report)

Approved for Public Release;
Distribution Unlimited

17. DISTRIBUTION STATEMENT (of the abstract entered in Block 20, if different from Report)

18. SUPPLEMENTARY NOTES

19. KEY WORDS (Continue on reverse side if necessary and identify by block number)

Nonspherical Particles
Scattering
Particle Sizing

20. ABSTRACT (Continue on reverse side if necessary and identify by block number)

Differential scattering patterns were photographically recorded from several types of nonspherical particles. Sizes were determined from the scattering patterns and compared with microscopically measured ones.

DD FORM 1 JAN 73 1473 EDITION OF 1 NOV 65 IS OBSOLETE

UNCLASSIFIED

SECURITY CLASSIFICATION OF THIS PAGE (When Data Entered)

I INTRODUCTION

The scattering of electromagnetic radiation has been studied since the days of Lord Rayleigh who first provided a theory[1] of scattering by small dielectric spheres in 1881. Since that time mathematical solutions to the general scattering problem have been found only for a very limited set of scatterer geometries; spheres by Mie[2] (1908), infinitely long cylinders by Wait[3] (1955), and prolate and oblate spheroids by Asano and Yamamoto[4] (1975). By general we mean a solution applicable to all particle sizes, relative to the wavelength of the radiation, and arbitrary optical parameters and orientations.

This state of affairs poses a problem for those working with real aerosols. Except for the case of aerosols composed of small liquid droplets, practical clouds are composed of irregular particles for which scattering solutions do not exist. This is especially true for the case of deliberate obscuration clouds where one wishes to exploit special properties of fibers or flakes. One form of the problem is that there is no convenient way of deducing the scattering pattern from a single particle so that the scattering from the cloud can be predicted or analyzed. Another facet of the problem is that of determining the size distribution of an aerosol. In general, the theory for the size-measuring apparatus is worked out for spheres and the instrument calibrated with spheres. The results of a measurement on non-spherical particles are not easily analyzed.

In this work we take an experimental approach to the problem of scattering from non-spherical particles. In particular, we measured the scattering patterns from individual particles of different kinds.

These were analyzed and compared with spheres to see if they differed significantly and if the scattering patterns could be used to distinguish classes, i.e., fibers from flakes, and sizes. The following section contains a description of the experimental procedure, Section III the results, and Section IV an analysis of these results.

II EXPERIMENTAL TECHNIQUE

The core of the particle measurement system is an electrodynamic balance for suspending single particles using electric fields. The theory of this device is given in a paper by Davis and Ray[5]. Figure 1 is a photograph of the system showing the slit through which

the scattering pattern is obtained as the dark line between the shiny electrodes. This scattering pattern is recorded on a piece of film wrapped around the suspension chamber in the configuration shown in Figure 2.

Film was chosen over a scanning electronic detector in spite of its smaller dynamic range for two compelling reasons. Time resolution was the principal. Visual observation of the scattering pattern revealed substantial changes over times of a few seconds due to random air currents disturbing the particles. Since mechanically scanning a detector would have taken 10's of seconds the scanned output would have been an indecipherable superposition of scattering patterns from many particle orientations. Film allowed the entire pattern to be recorded in times of 1/50 to 1/100 second, eliminating the motion problem. In addition, film allowed us to record the scattering pattern in a 5.5^{o} arc around the beam as well as a 168^{o} arc measured from the beam axis, thus a limited amount of two-dimensional information was obtained.

For illumination the focused beam from a 50 mw HeNe laser operating at a wavelength of 632.8 nm was used. The observed scattering plane was horizontal and the laser was linearly polarized perpendicular to this plane. As no polarization filter was used in front of the film, the recorded scattering pattern is the sum of both perpendicular and parallel polarization components of the scattered radiation.

The suspended particles were observed with a long working distance microscope (60X magnification, resolution 6μm) using backlighting with white light. The entire chamber was rotated so that the particle could be observed from the same direction as the incident laser beam. In general, the particles oriented themselves so that their longest dimension was vertical. The asymmetric ones tended to maintain equilibrium positions about this axis. However, random air currents would sometimes cause them to rotate several degrees about the vertical axis before they returned to the equilibrium position. As it was not possible to simultaneously observe the particle and record a scattering pattern, there is uncertainty as to the rotational orientation of the particle for a given scattering pattern. We are searching for ways to eliminate this ambiguity. The sketches that accompany the scattering patterns in the next section show the particles in the equilibrium configuration.

III EXPERIMENAL RESULTS

Particles for these experiments were chosen on the basis of four criteria: material or shape of interest, readily available, as small as possible subject to the constraint that they must be observable in the long working distance microscope, and must acquire enough static charge during normal handling to be suspended in the electrodynamic balance. The third condition effectively limits the smallest particle dimension to 6 μm, the resolution limit of the microscope. This is somewhat larger than desirable as typical aerosols tend to have dimensions on the order of 1 μm. It is planned that future versions of this system will have the capability of working with these smaller particles. Six types of particles, described below, were selected for this series of measurements.

Glass - spheres 25 to 30 μm in diameter with an index of refraction of 1.525.

Aluminum - irregular flakes 10 μm thick and on the order of 100 μm in the other two dimensions.

Stainless steel - fibers 8 μm in diameter and about 200 μm long.

Carbon - nearly spherical particles 30 to 50 μm in diameter.

Carbonyl iron - irregular agglomerates, 10 to 30 μm in size, formed from 1 μm spheres.

Salt - nearly cubic crystals 20 to 30 μm in size.

Electron micrographs of these samples are shown in Figures 3-8.

The data from this experiment consist of a set of photographs of scattering patterns. These will be presented in a systematic fashion so that comparisons can be made between different classes of particles. First in each series of figures will be a sketch of three particles from each class in their equilibrium position. Following this will be the scattering patterns from these three particles arranged in the same order. The final figure of each series will be three scattering patterns from the same particle, the one in the center of the preceding figures, so that time variation of the patterns can be seen.

In each photograph of a scattering pattern the left hand edge of the pattern is 6.0 degrees from the beam direction and the righthand edge corresponds to 174 degrees. Figures 9-11 show the data for the glass spheres. The sharp, evenly spaced fringes predicted by Mie theory are clearly visible. The next set, Figures 12-14, are for aluminum flakes. A beacon like effect, most easily seen in Figure 14, is the result of the large, relatively flat surface of these objects. In the pattern for stainless steel fibers, Figures 15-17, one can see a few broad, vertical fringes representative of the 8 μm diameter of the fiber and a very fine horizontal pattern reflecting the length. Carbon near-spheres, Figures 18-20, show a pronounced regular fringe pattern corrupted by interference effects. The patterns from the agglomerate, carbonyl iron particles, Figures 21-23, show very coarse structure characteristic of their small size. Finally, scattering data for salt crystals are shown in Figures 24-26. In the following section we will analyze these data to obtain some quantitative information on the particles.

IV ANALYSIS

As was pointed out in the introduction no general solutions exist for predicting scattering from the particles used in this study except for the spheres. Thus, our analysis must be of an approximate nature. The approach chosen was to treat the particles as totally absorbing, two-dimensional objects and determine their size from the data using Fraunhofer diffraction theory.[6] From Babinet's principle the off-axis scattering of this object is the same as for a screen with a complementary aperture. Both the square and circular apertures asymptotically satisfy the following relationship (see Ref. 6).

$$\text{size} = \frac{\text{wavelength}}{\text{angular spacing of minima}} \qquad (1)$$

We generalize this relationship, without rigorous proof, for the particles used in this experiment. Sizes, shown in Table I, were determined in the following manner. Scattering patterns were examined visually in the 10° to 45° region to find what appeared to be a series of regularly spaced minima. This series was then measured with a set of calipers using as many minima as possible to obtain the best average value of the spacing. Two measurements were made on each film strip to estimate the reproducibility of the results. The standard deviation between the size as calculated from Equation (1) and the

Table I. Measured Particle Size

Pattern	No. of Spacings	Length of Series[1]	Size[2]	Microscope Size[3]
Fig. 10, #2	20	1.388	22.3	24
Fig. 10, #2	19	1.312	22.4	24
Fig. 10, #3	29	1.576	28.5	30
Fig. 10, #3	22	1.184	28.7	30
Fig. 16, #3	3	.601	7.7	8
Fig. 16, #3	2	.405	7.6	8
Fig. 16, #2	2	.350	8.8	8
Fig. 16, #2	2	.359	8.6	8
Fig. 19, #1	11	.522	32.6	30
Fig. 19, #1	9	.432	32.2	30
Fig. 19, #2	9	.325	42.8	36
Fig. 19, #2	9	.328	42.4	36
Fig. 22, #2	2	.360	8.6	12
Fig. 22, #2	2	.364	8.5	12
Fig. 22, #1	2	.231	13.4	12
Fig. 22, #1	2	.226	13.7	12
Fig. 25, #3	6	.408	22.7	30
Fig. 25, #3	7	.493	22.0	30
Fig. 25, #2	3	.341	13.6	24
Fig. 25, #2	2	.248	12.5	24

1) Dimensions are in inches. The film was formed into an arc with radius 2.443".

2) Dimensions are in micrometers. The laser wavelength was 0.6328 μm.

3) Dimensions are in micrometers. Consideration of microscope resolution and reticle spacing leads to an estimation of 6 μm as the uncertainty in the microscopically determined size.

microscopically determined size is 4.9 μm, less than the 6 μm uncertainty in the microscope measurements. The aluminum flakes were excluded from this analysis as their large size made the minima spacings too small for accurate counting and measuring with the technique used.

Despite this statistical agreement there is evidence that the use of Equation (1) in size determination should be approached with caution. Mie theory calculation[7] for the glass spheres show that spheres 25.7 μm in diameter give the 1.63° spacing between minima that was measured for the first sphere in Table I. The size calculated from Equation (1) is 22.3 m, a 13% error.

V CONCLUSIONS

The principal conclusion to be drawn from this work is qualitative. The scattering patterns, Figures 9-26, show that differently shaped particles have characteristic patterns. These can be used to identify different geometric classes, i.e., fibers and flakes. A simple analysis based on fringe spacing also shows that approximate size information is contained in these patterns and that better microscopically measured sizes are necessary to critically test this method. In summary, the scattering pattern for particles in the 8 to 40 m size range contains accessable information on particle size and shape.

REFERENCES

1) Lord Rayleigh, Phil. Mag. 12, 81 (1881).

2) G. Mie, Ann. Physik. 25, 377 (1908).

3) J. R. Wait, Can. J. Phys. 33, 189 (1955).

4) S. Arans and G. Yamamoto, Appl. Opt. 14, 29 (1975).

5) E. J. Davis and A. K. Ray, J. Colloid and Interface Sc. 75, 566 (1980).

6) Principles of Optics, M. Born and E. Wolf, Pergammon Press, Oxford, 1975.

7) J. V. Dave, Subroutine for Computing the Parameters of the EM-Radiation Scattered by a Sphere. IBM Document No. 360D-17.4.002, IBM Scientific Center, Palo Alto, CA (1968).

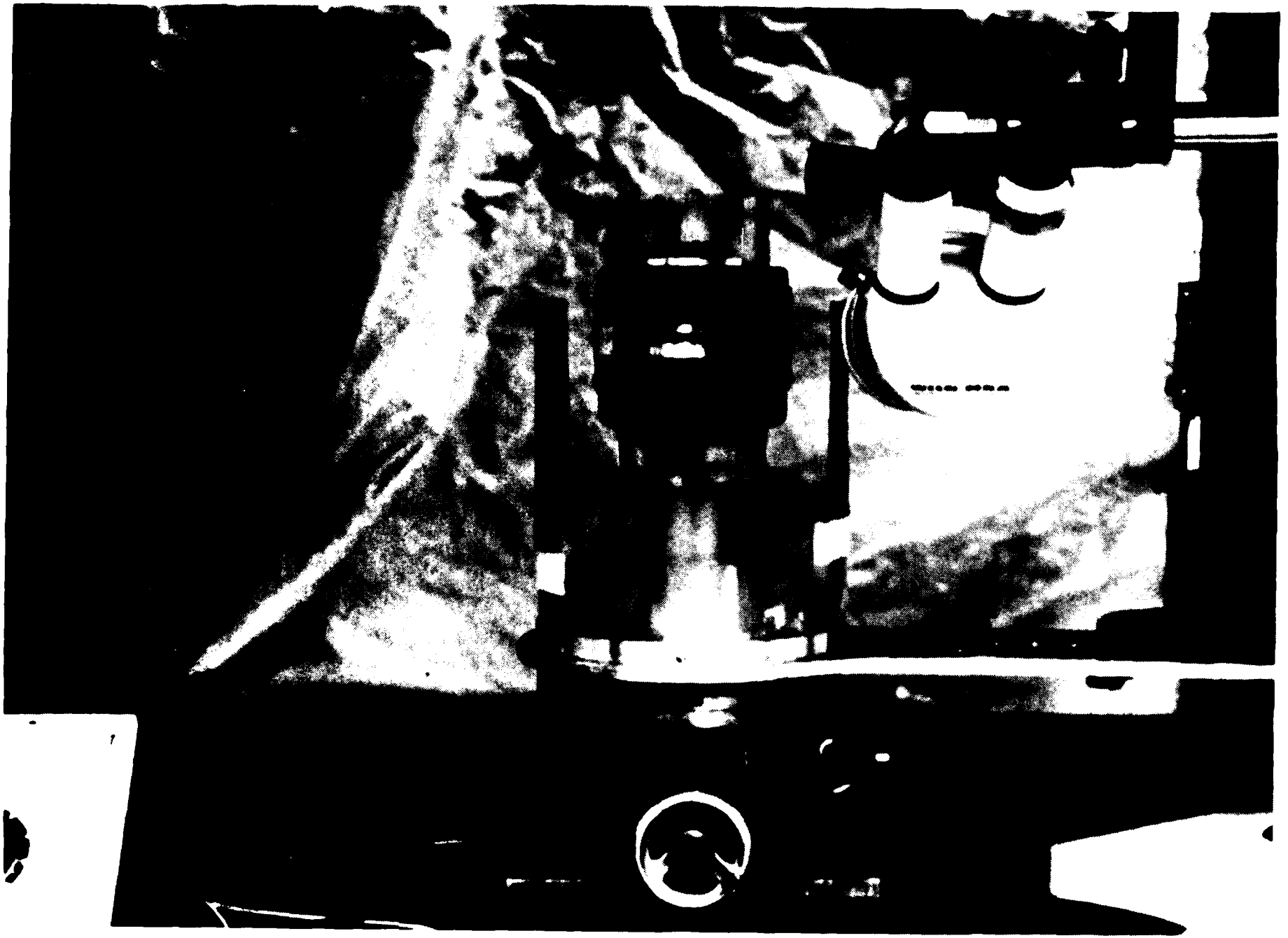

Figure 1 Photograph of electrodynamic balance.

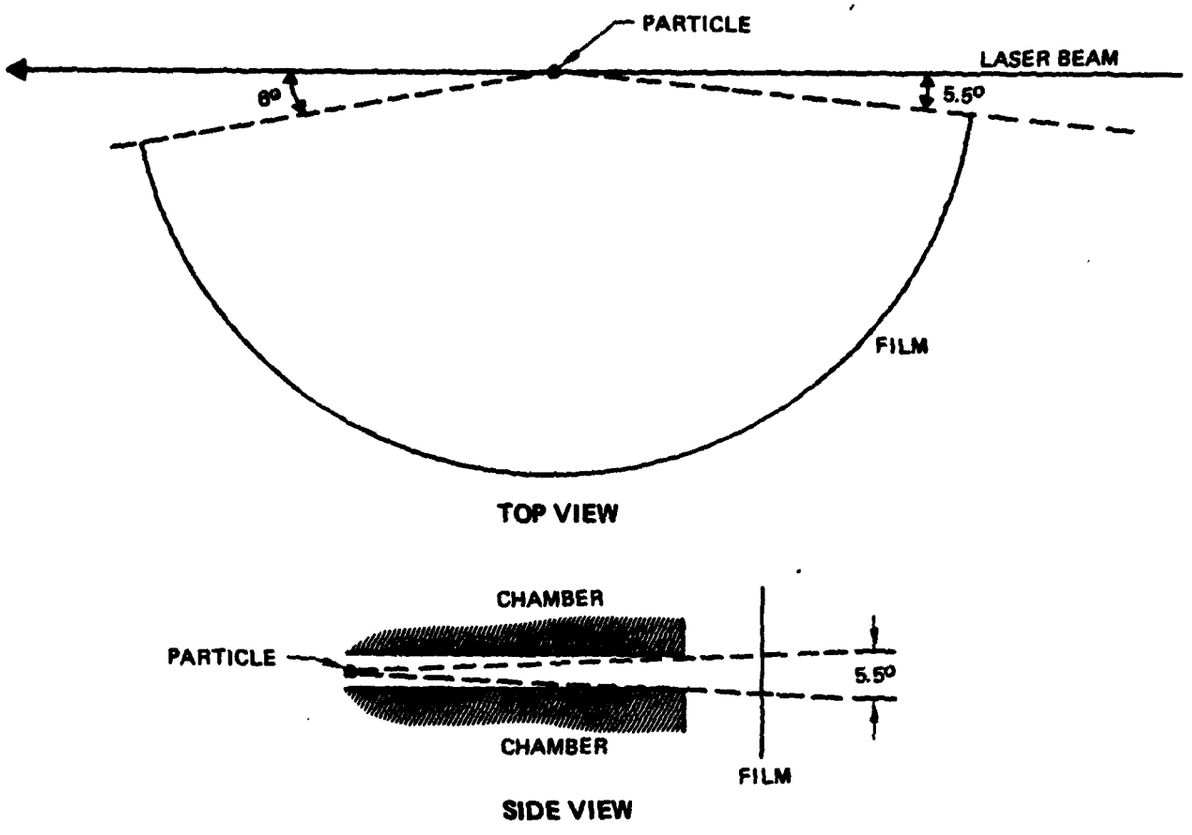

Figure 2 Film geometry.

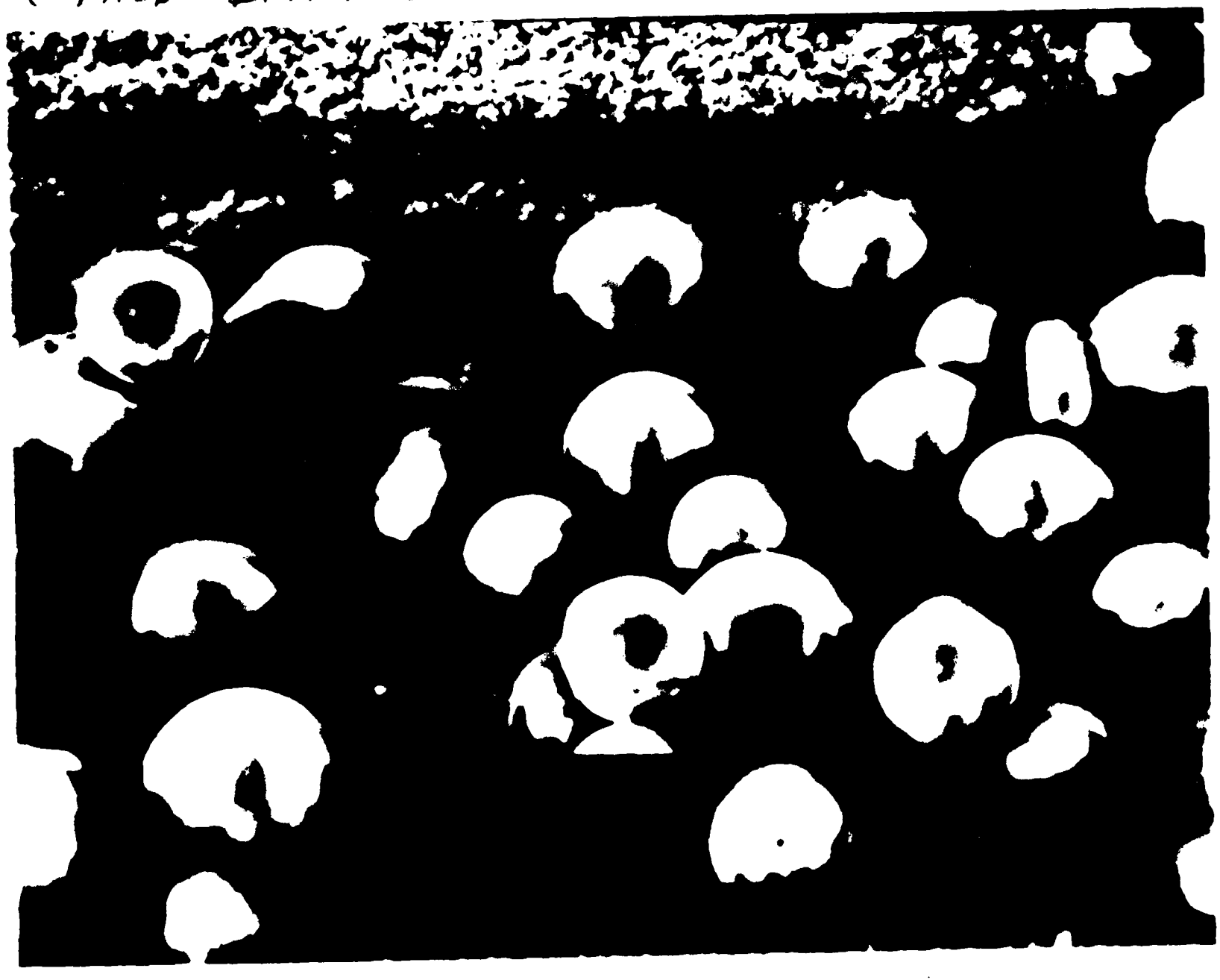

Figure 3 Glass spheres.

Figure 4 Aluminum flakes.

Figure 5 Stainless steel fibers.

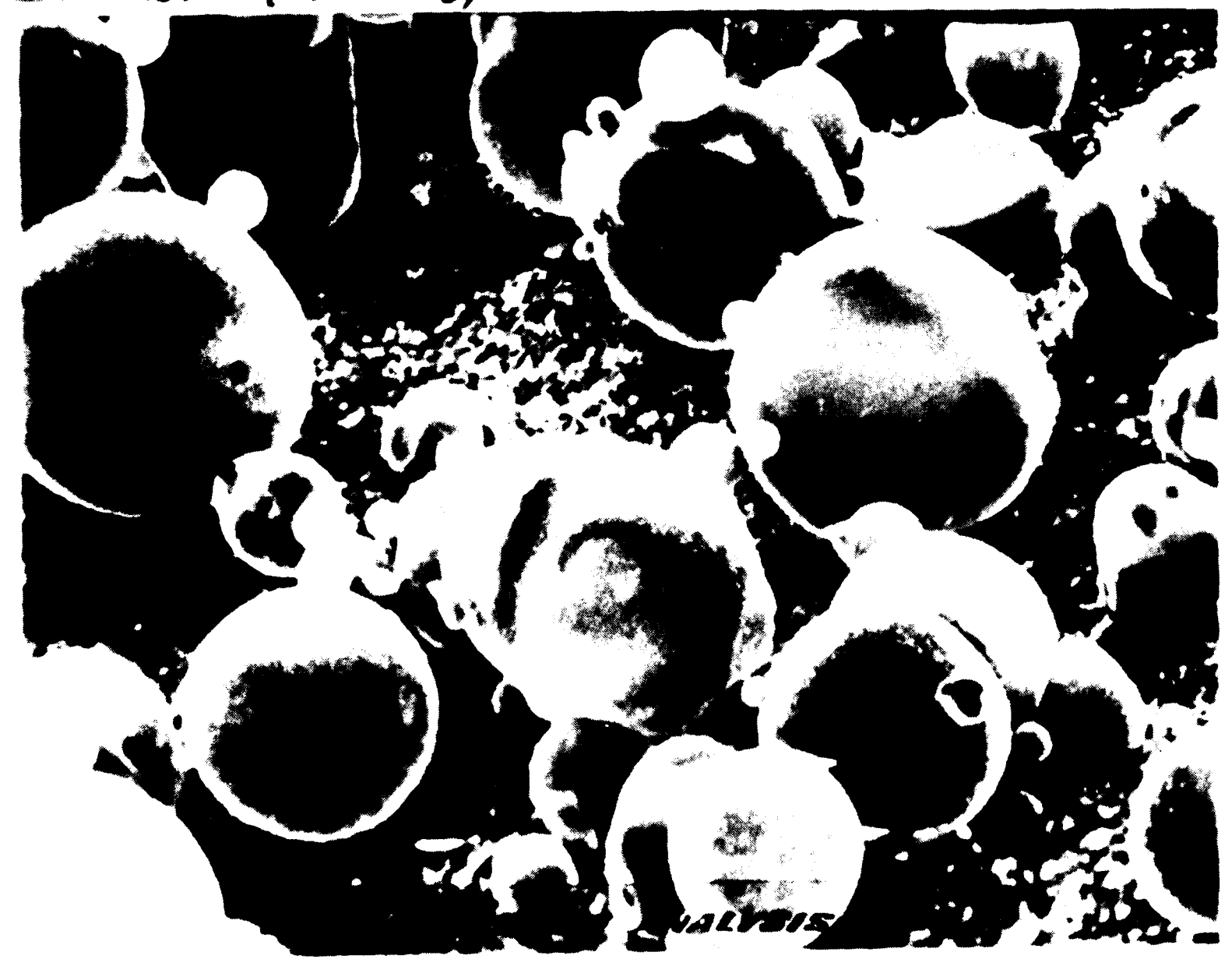

Figure 6 Carbon near-spheres.

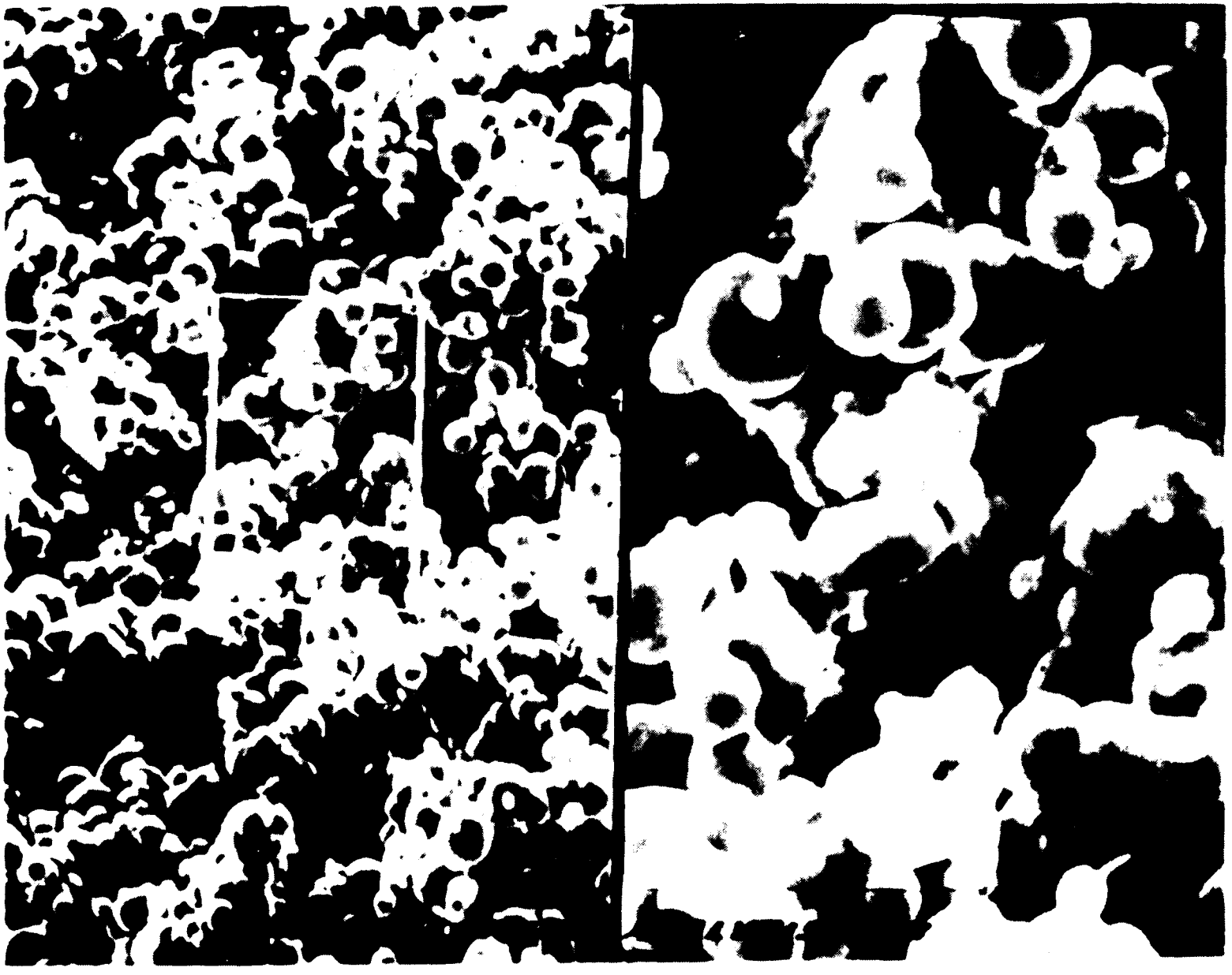

Figure 7 Carbonyl iron agglomerates.

Figure 8 Salt crystals.

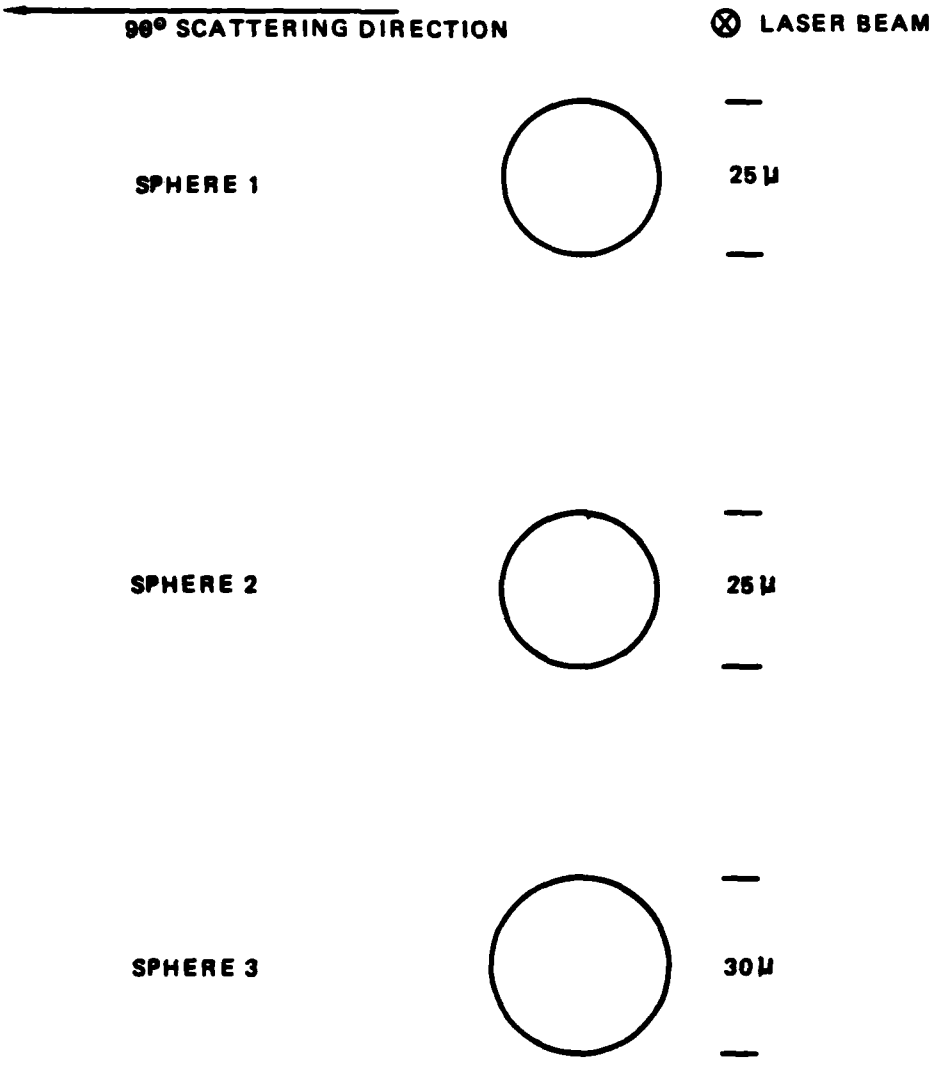

Figure 9 Sketch of glass spheres.

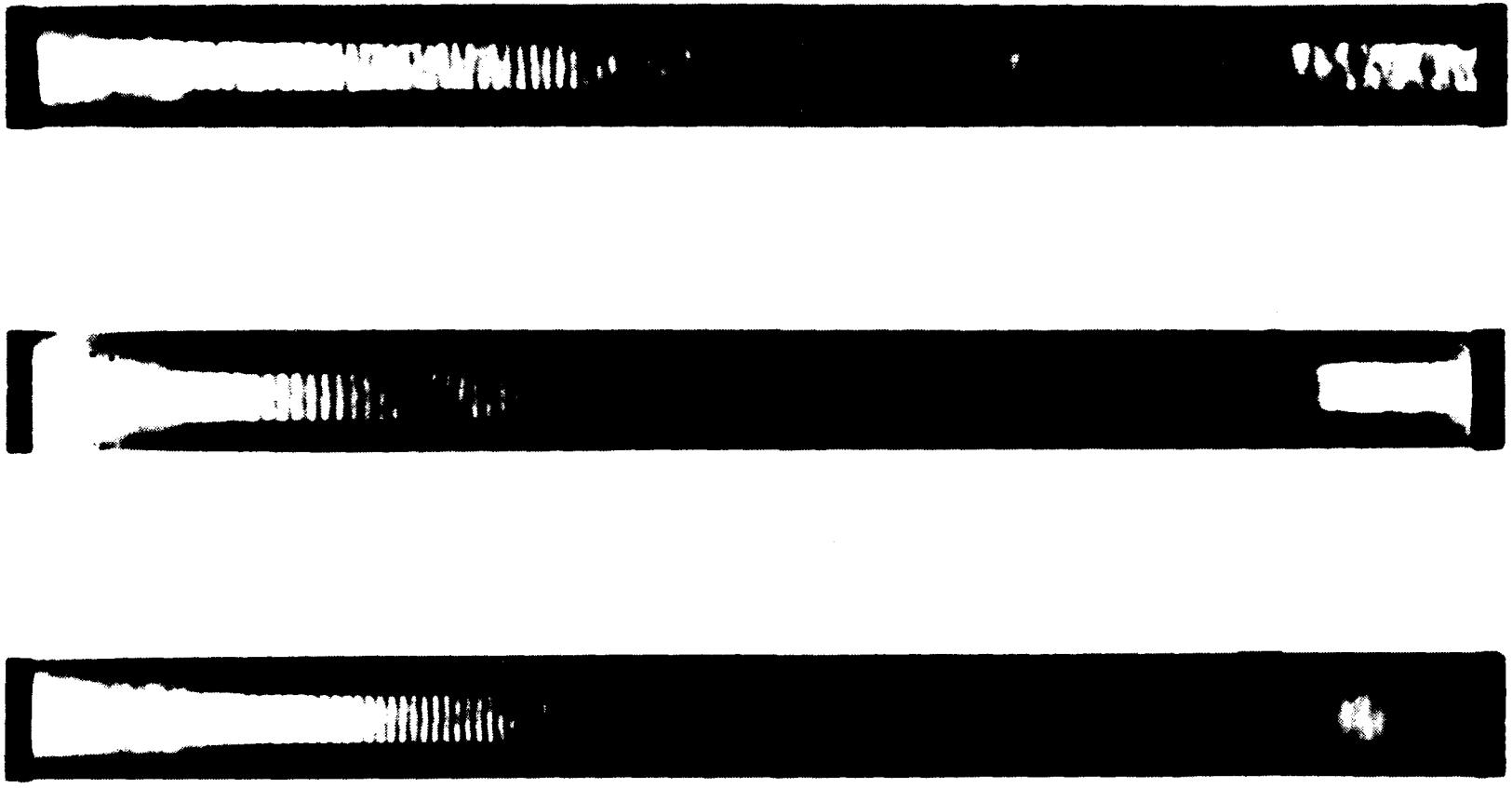

Figure 10 Scattering patterns for three spheres.

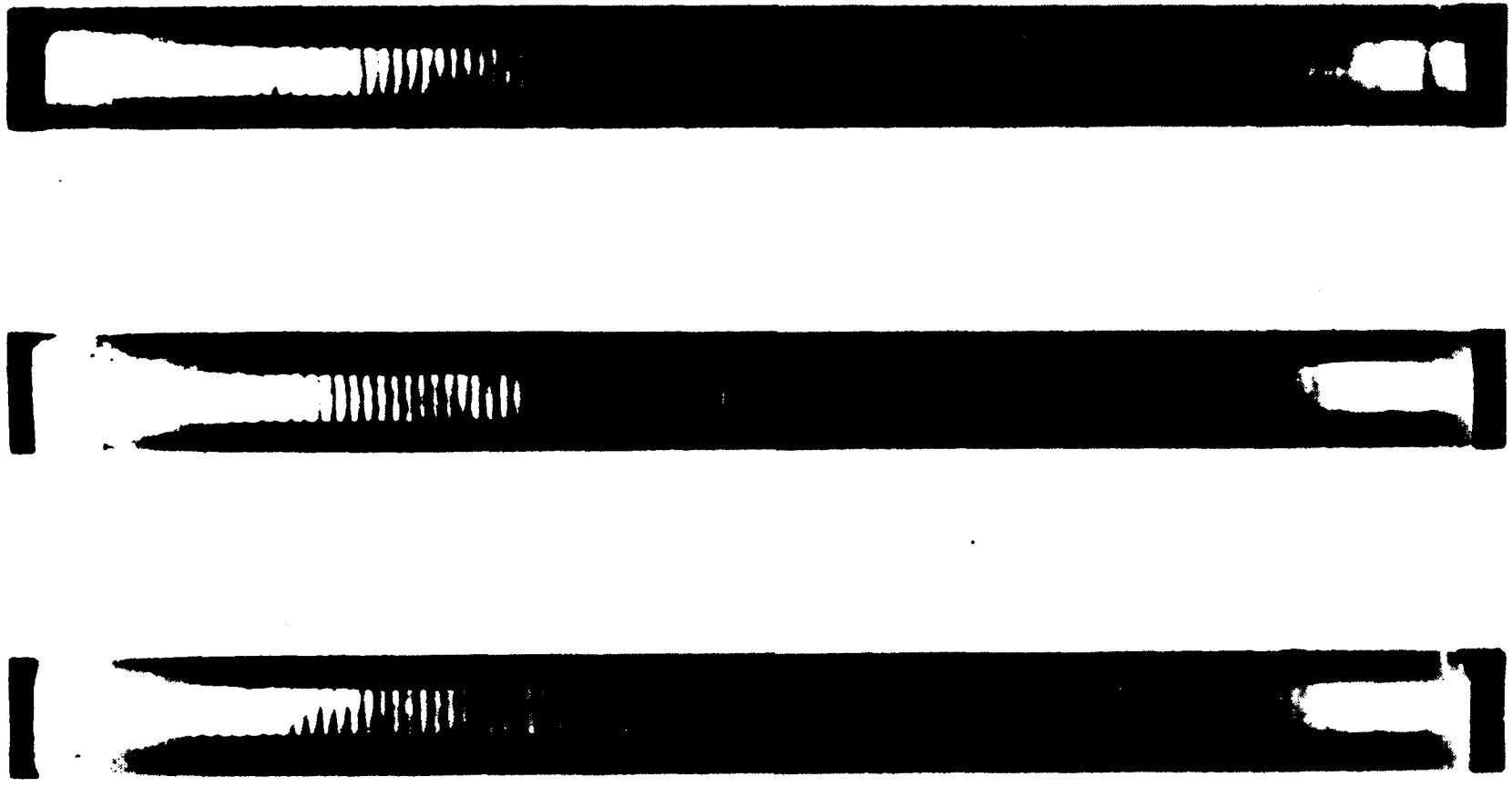

Figure 11 Scattering patterns for sphere #2.

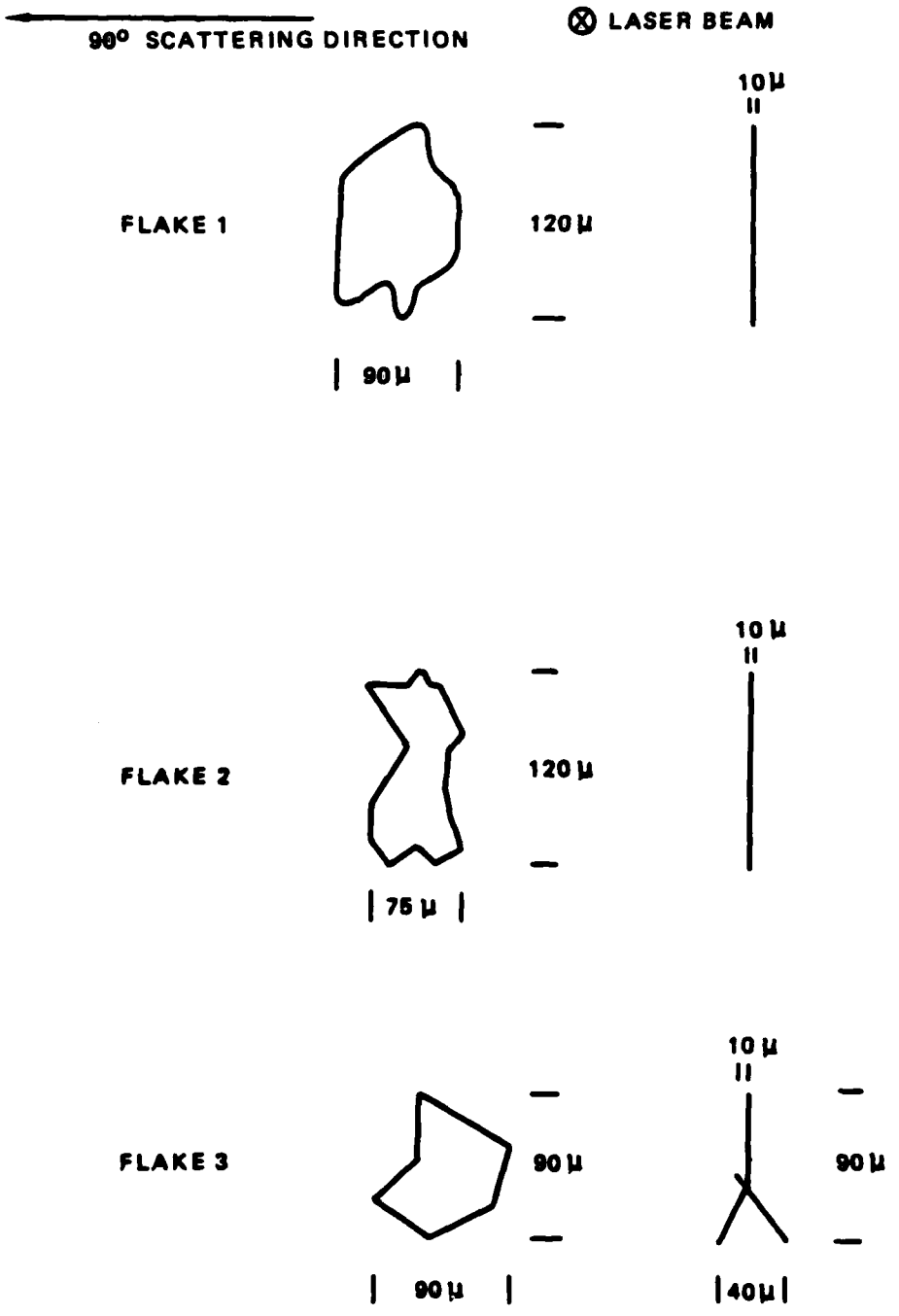

Figure 12 Sketch of aluminum flakes.

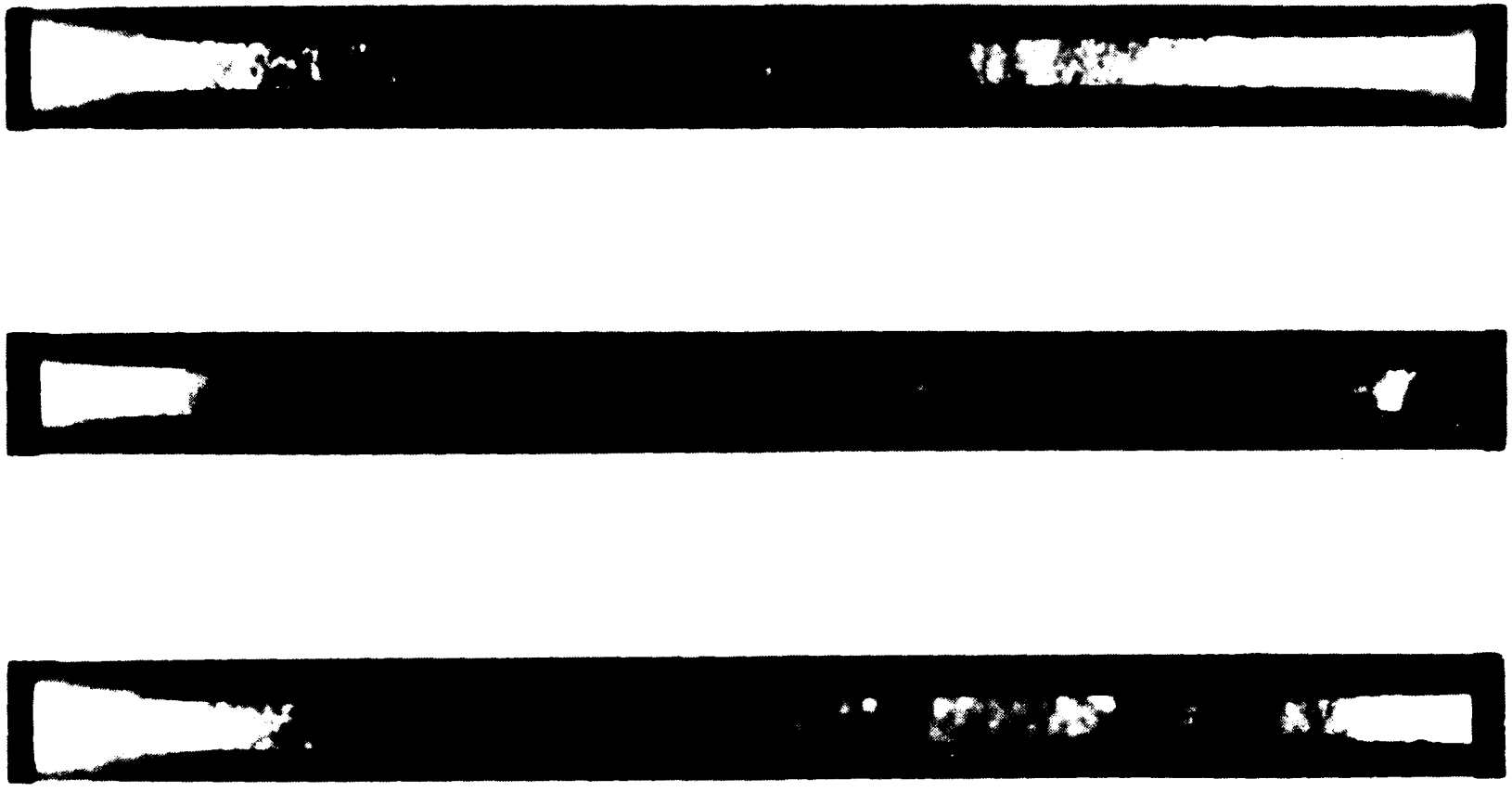

Figure 13 Scattering patterns for three flakes.

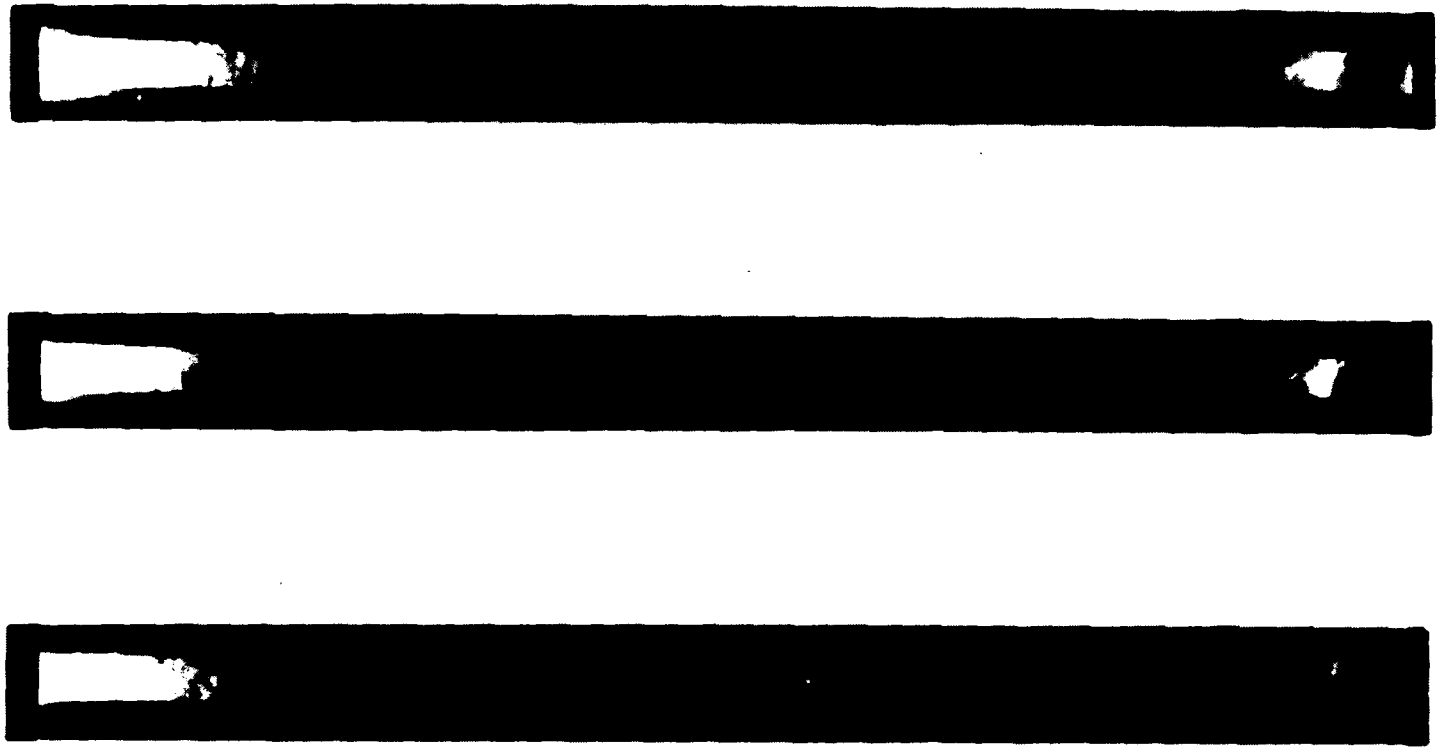

Figure 14 Scattering patterns from flake #2.

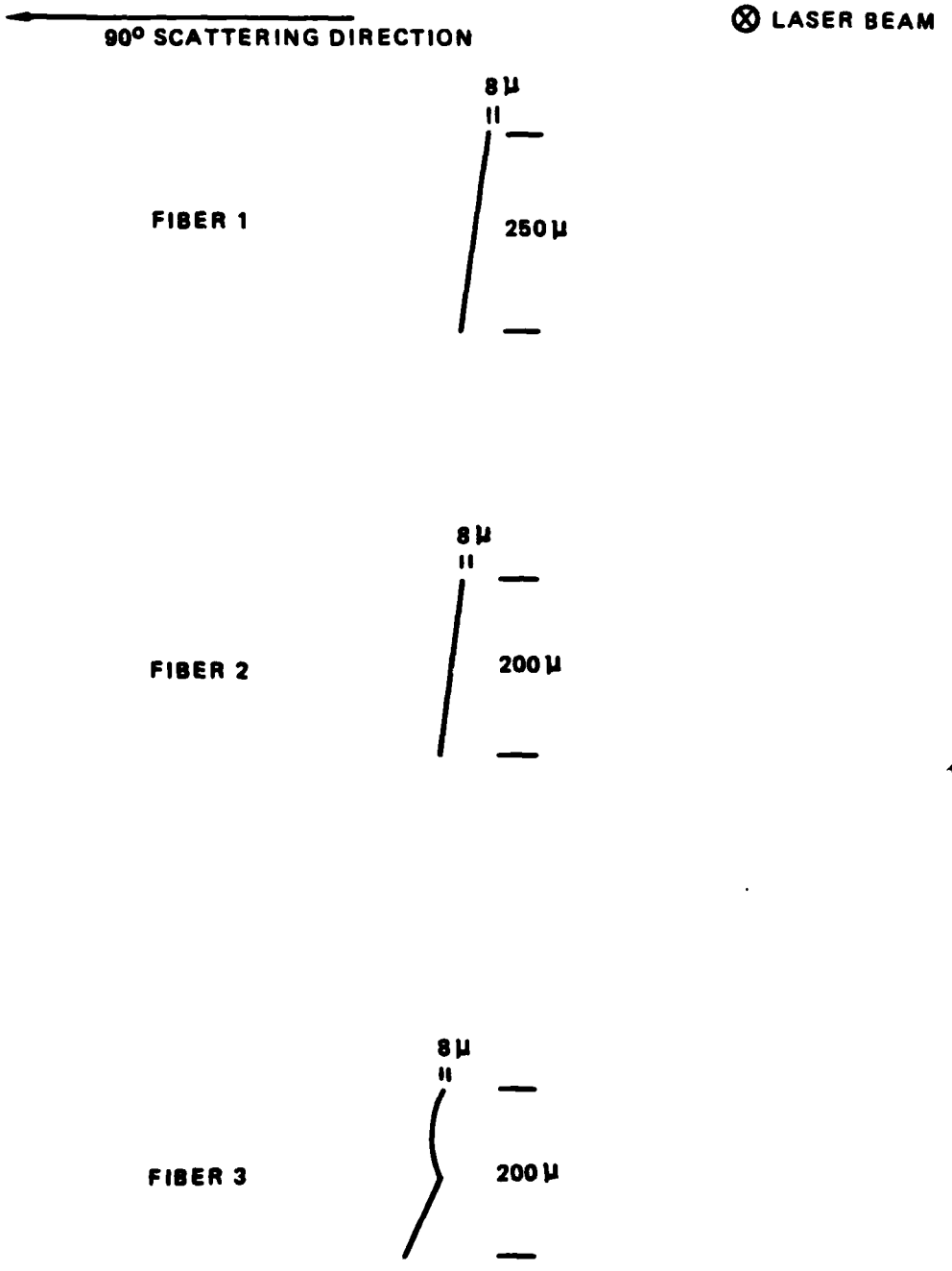

Figure 15 Sketch of stainless steel fibers.

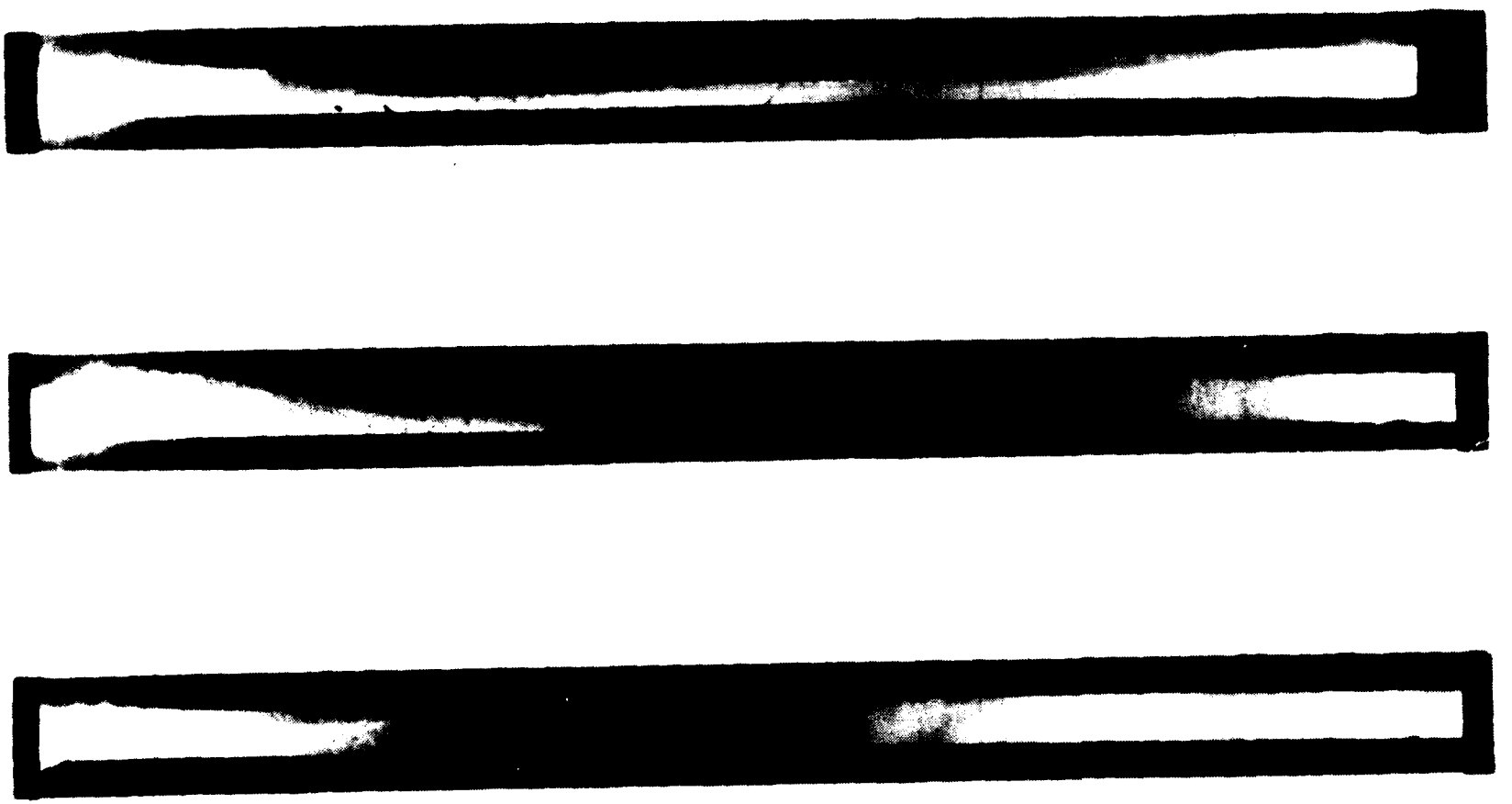

Figure 16 Scattering patterns for three fibers.

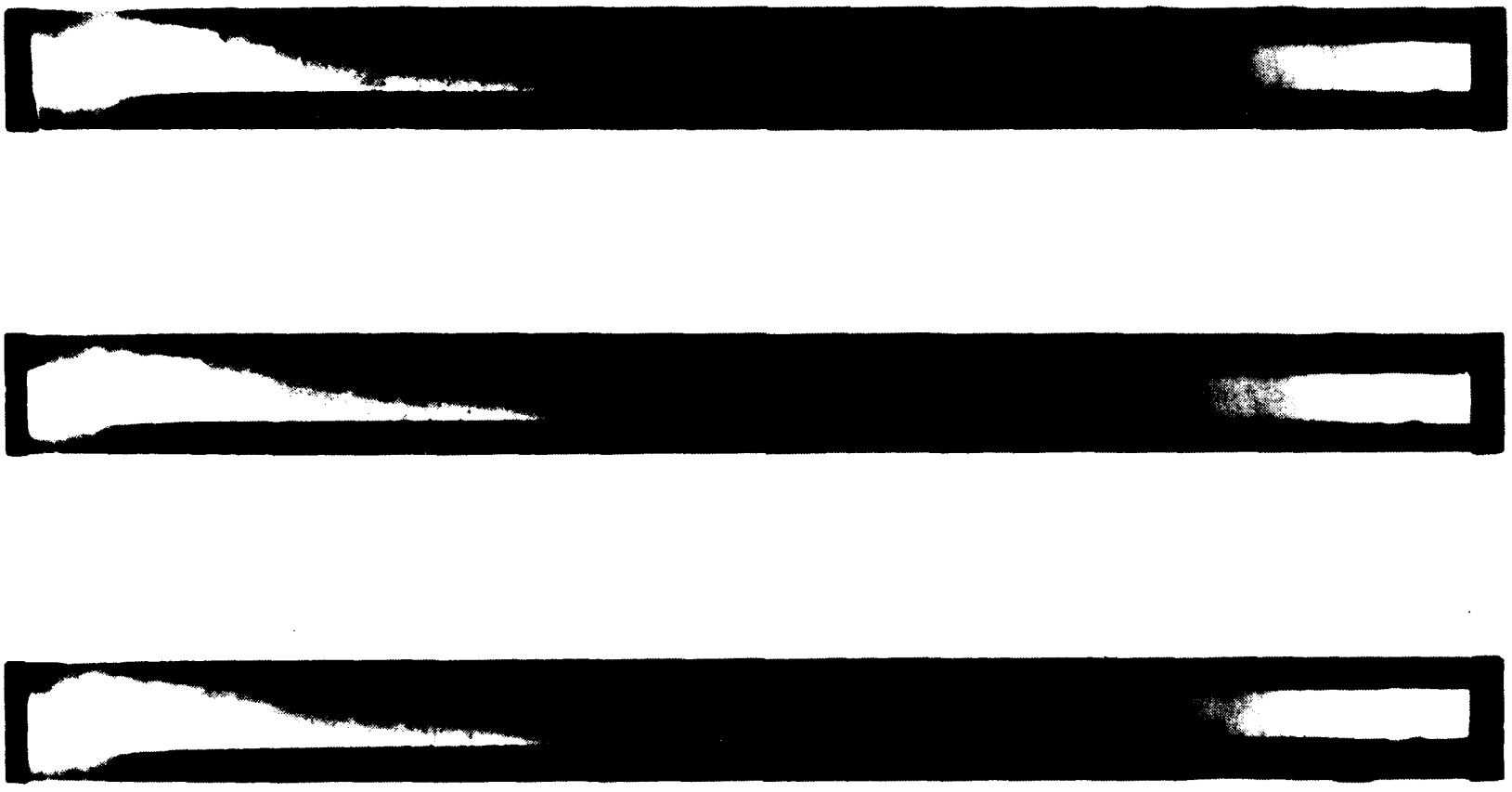

Figure 17 Scattering patterns from fiber #2.

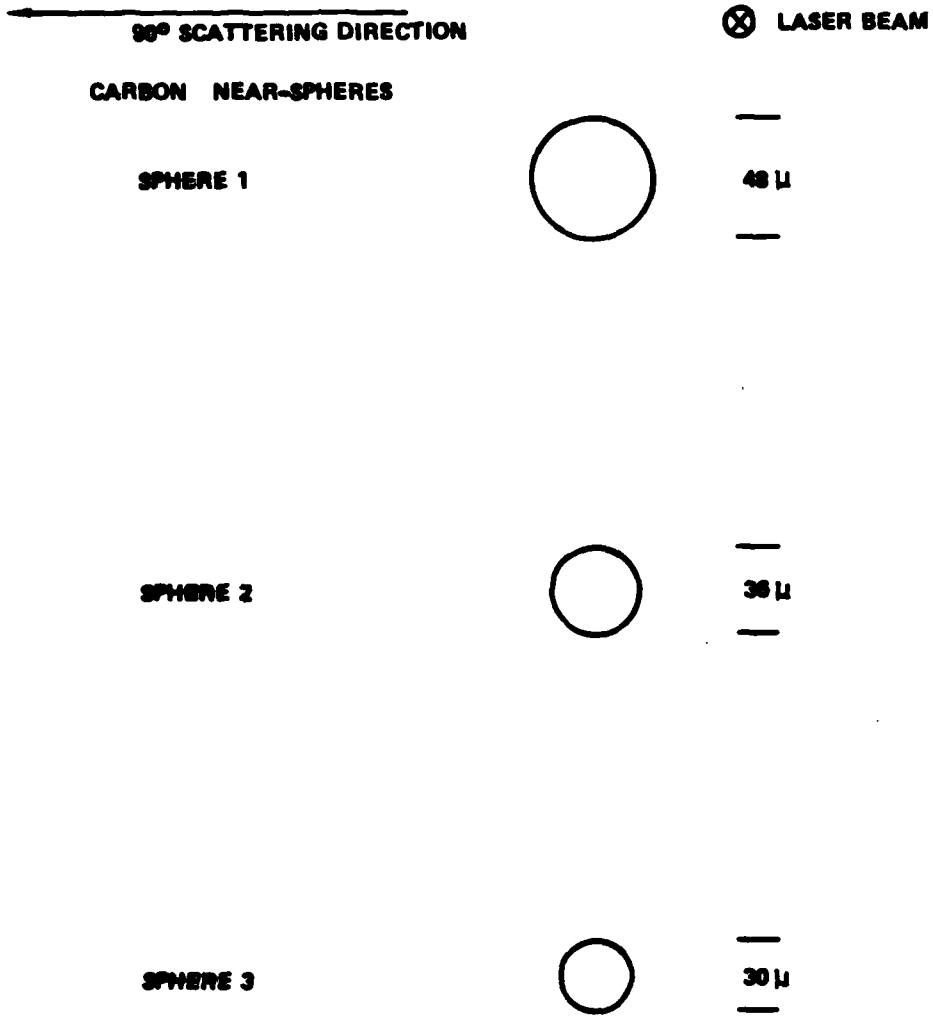

Figure 18 Sketch of carbon near-spheres.

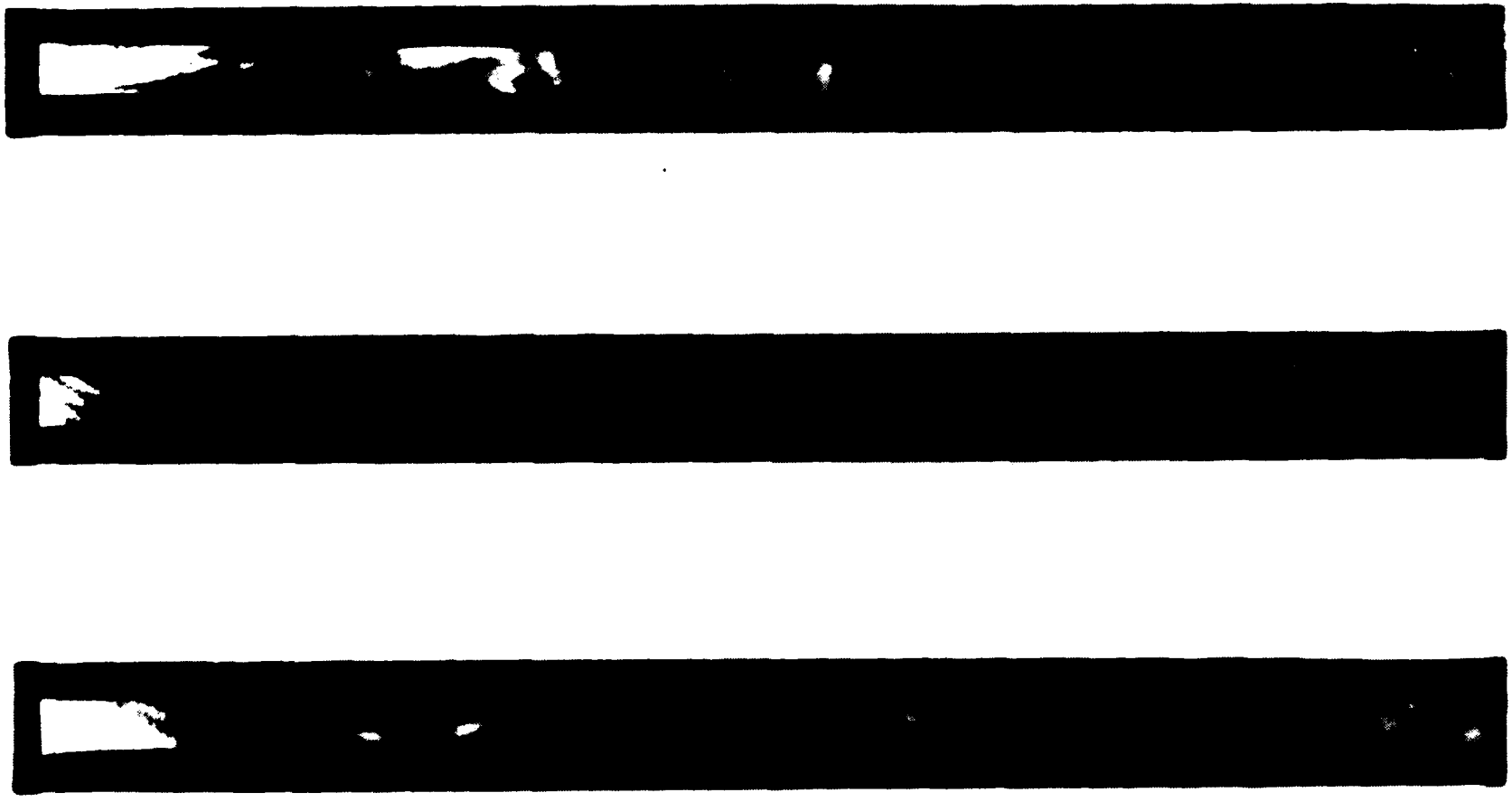

Figure 19 Scattering patterns for three near-spheres.

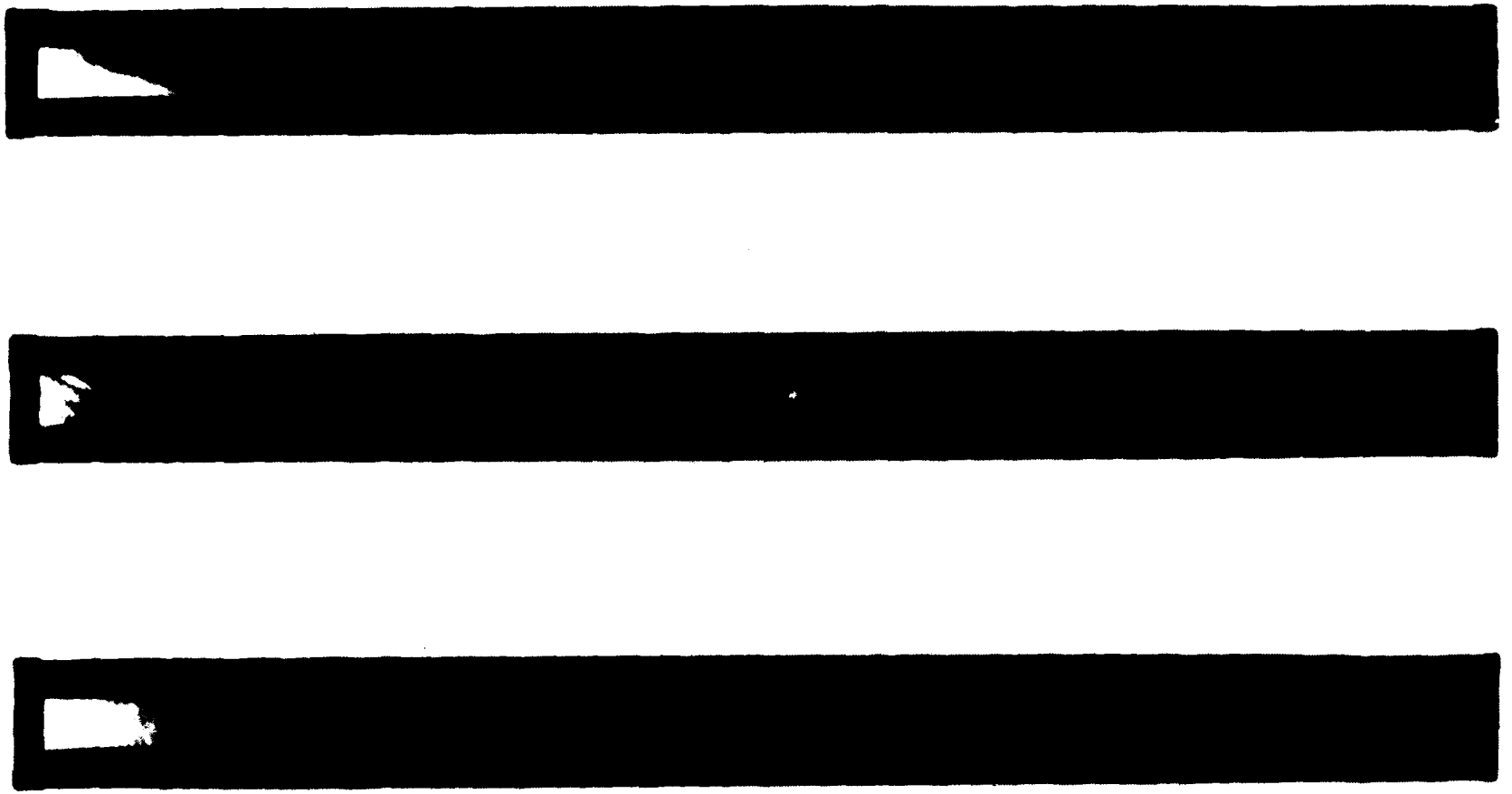

Figure 20 Scattering pattern from near-sphere #2.

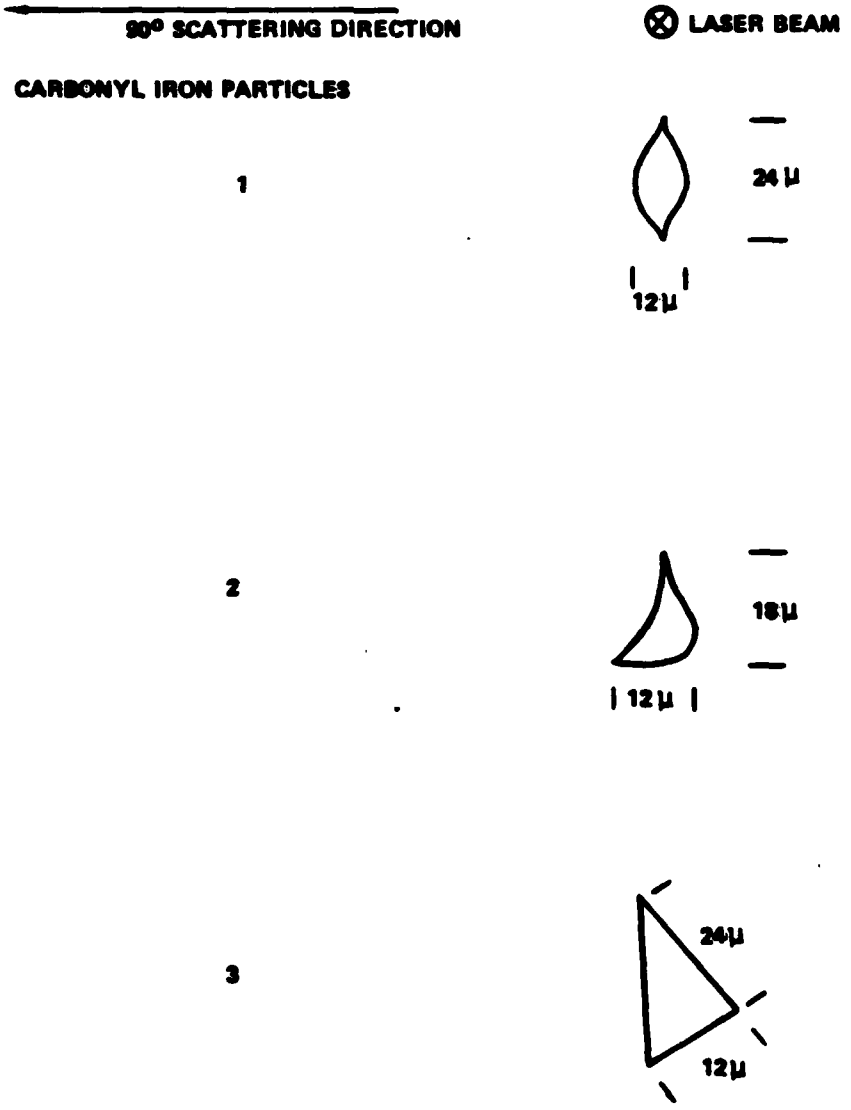

Figure 21 Sketch of carbonyl iron agglomerates.

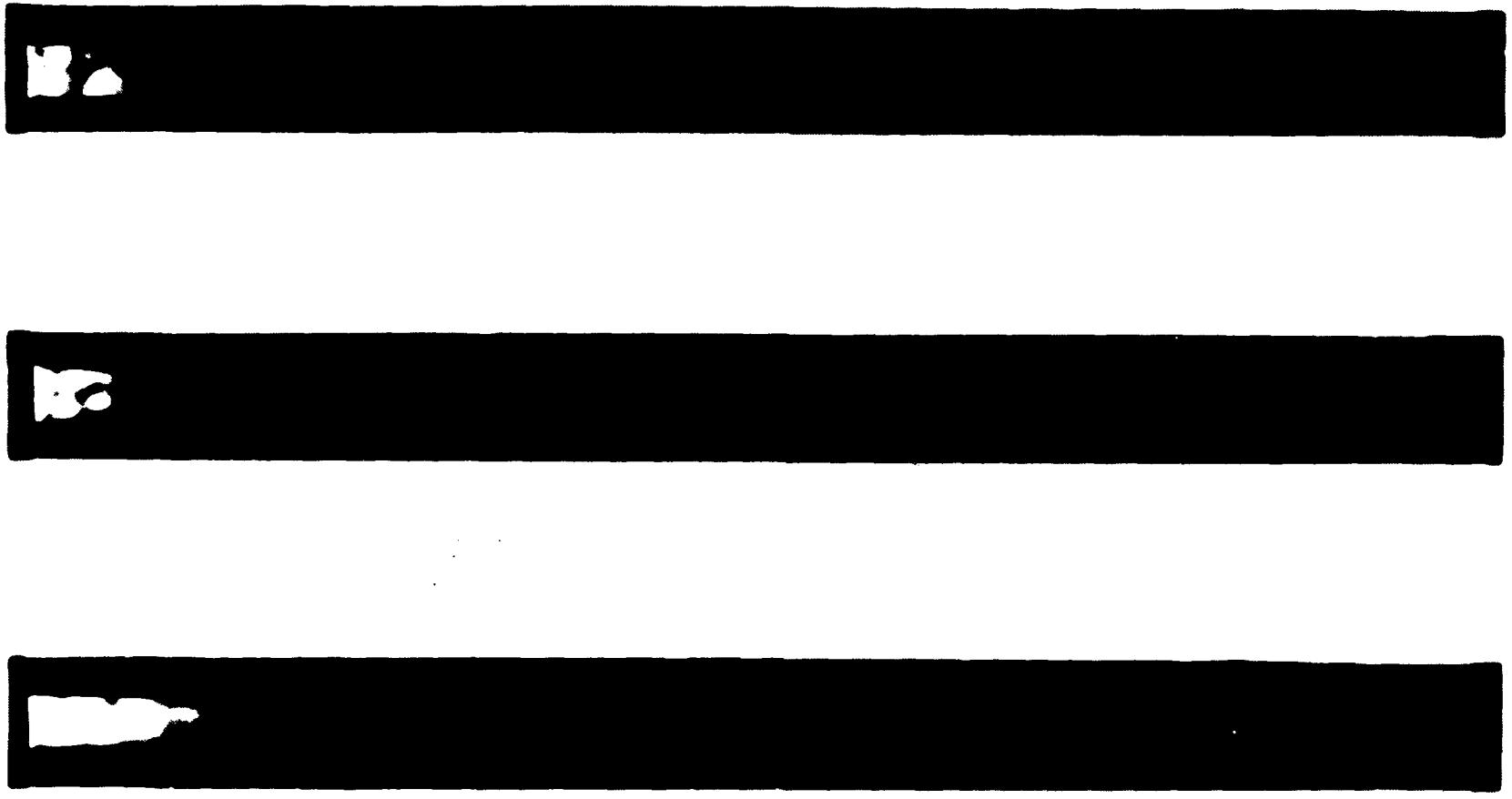

Figure 22 Scattering patterns for three agglomerates.

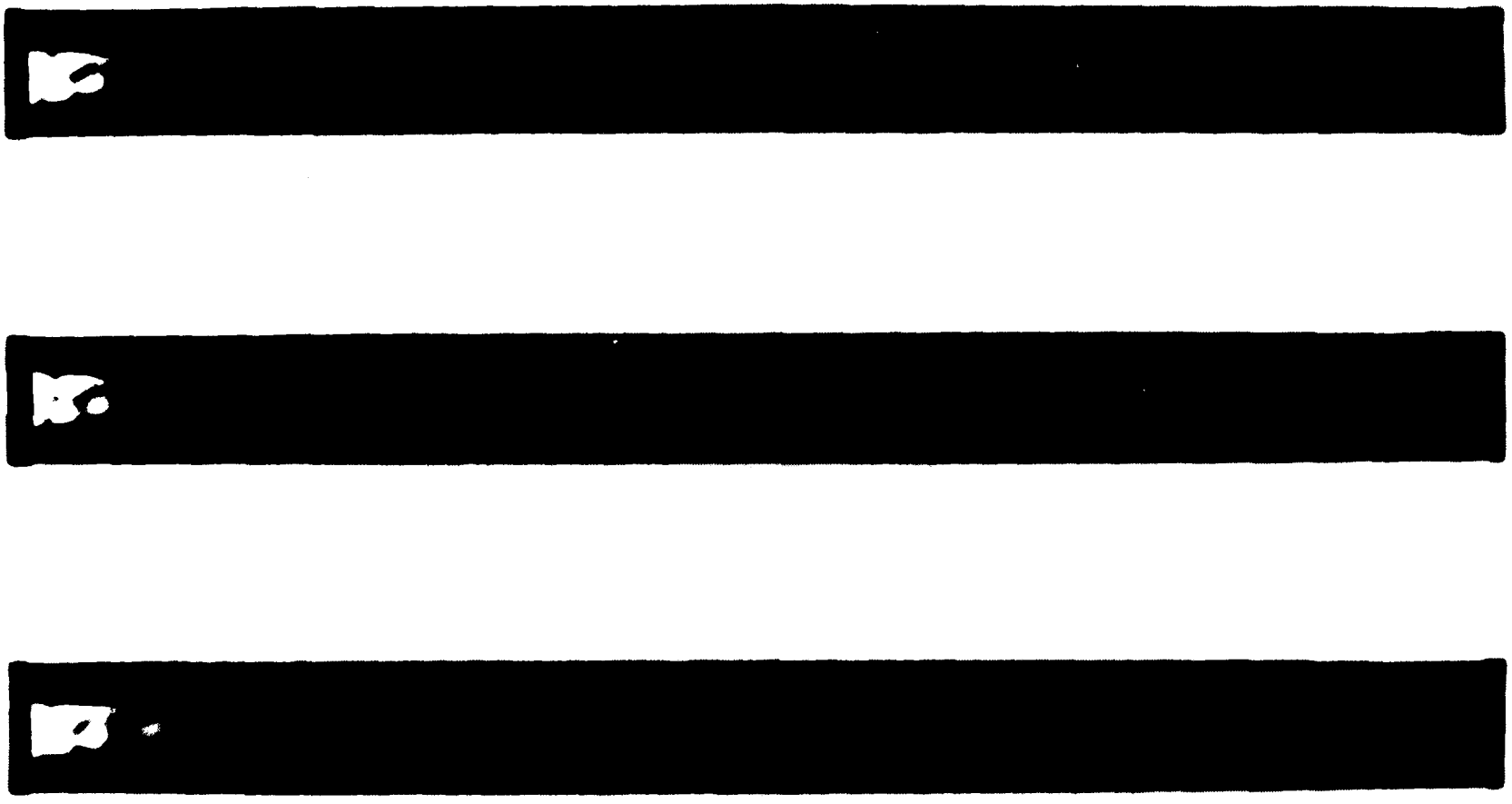

Figure 23 Scattering patterns from agglomerate #2.

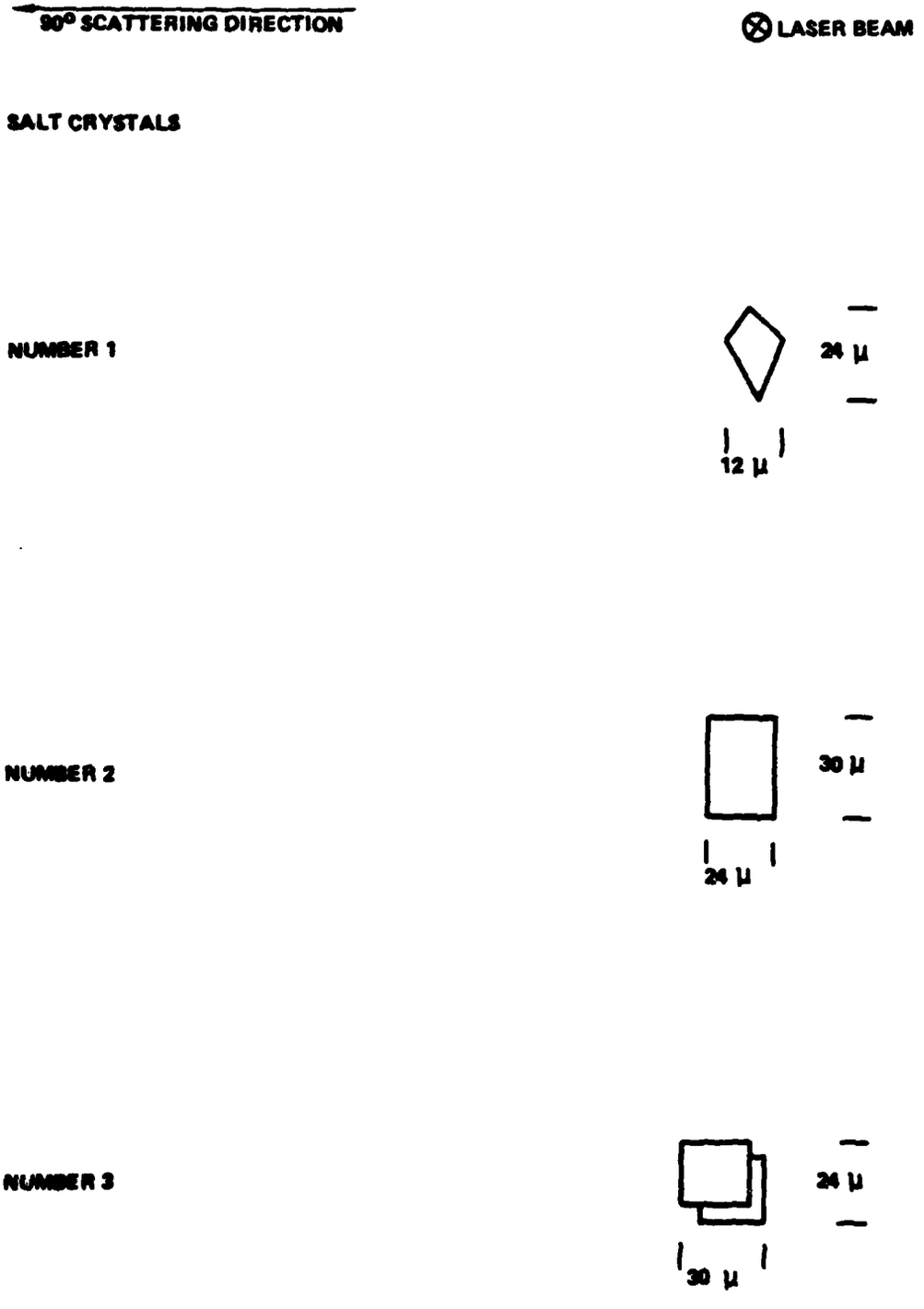

Figure 24 Sketch of salt crystals.

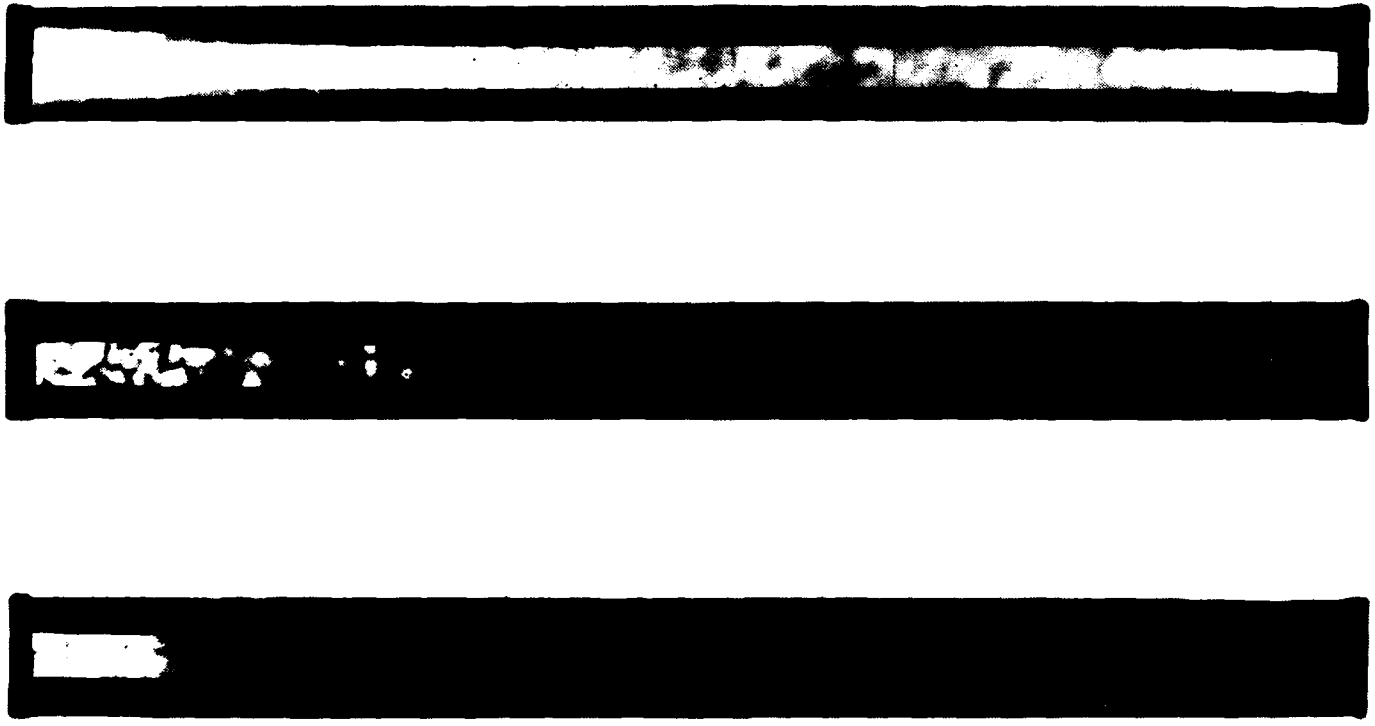

Figure 25 Scattering patterns for three crystals.

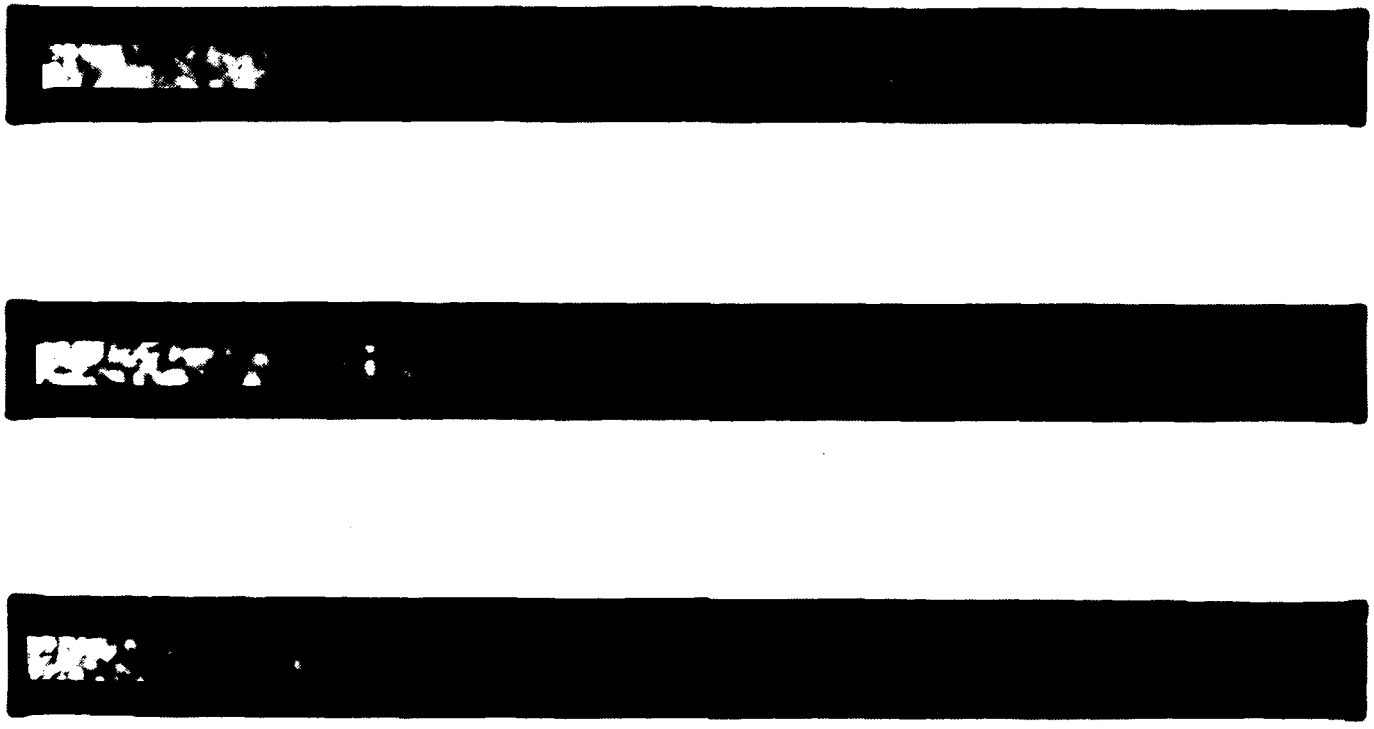

Figure 26 Scattering patterns from crystal #2.